

Validity on radar observation of middle- and upper-atmosphere dynamics

Susumu Kato

Professor Emeritus, Kyoto University, Uji, Kyoto, Japan

(Received July 27, 2007; Revised August 19, 2008; Accepted December 12, 2008; Online published May 14, 2009)

Doppler radar observations have made a large contribution towards improving our understanding of middle- and upper-atmosphere dynamics. This radar echo is mainly due to radiowave scattering by atmospheric turbulence, which occurs almost universally throughout the atmosphere as a result of gravity wave (GW) breaking. In the strictness sense, the radar pulse is back-scattered by radio refractive index (RRI) perturbations caused by turbulence whose size along the radar beam is half of the radar wavelength. Understanding of the validity of the MST (mesosphere, stratosphere and troposphere)-radar observation requires a precise knowledge of how RRI perturbations are formed and behave. A basic property of the RRI of the atmosphere is that it has a static vertical gradient in terms of distribution and the turbulence velocity is divergence-free. The RRI depends on three atmospheric properties—humidity, air density and electron density. These three elements each have a static vertical gradient along which turbulence transports each element, hereby perturbing the density distribution of each element; that is to say, it produces the RRI irregularity for scattering the radar pulse. Since the turbulence motion and winds are divergence-free, PRI perturbation co-moves with the total air flow, i.e. turbulence motion plus winds. This can be true even in the mesosphere where the perturbation is controlled electromagnetically. Co-movement of turbulence with local winds has been shown from a comparison of observations with radars and radiosondes. In addition to tracking turbulence as wind-tracers, MST-radar observations provide important data in the study of atmosphere turbulence dynamics.

Key words: Radio refractive index perturbations, turbulence, Doppler radar observations, atmospheric turbulence dynamics.

1. Introduction

Doppler radar echoes from the mesosphere were first detected by the Jicamarca radar in the 1970s (Woodman and Guillen, 1974). The echoes were subsequently determined to be due to scattering by atmospheric turbulence which co-moves with local winds. This finding paved the way to the radar observation of winds in the MST region (the mesosphere, stratosphere and troposphere) (Kato, 2005).

However, it has become necessary to critically review the principle of these radar observations of winds in the MST region as their validity has been taken for granted without any verification of the underlying assumptions for the observations. The aim of this review is provide a precise explanation of how the radar echoes are produced and how they behave in the presence of atmospheric turbulence. The radar echo can never be received from a uniform and incompressible medium (a current assumption), even in the presence of turbulence. The radar pulse is scattered by the radio refractive index (RRI) fluctuations in humidity, neutral air density and electron density. Although different approaches have been used to study the coupling between RRI fluctuation and the turbulence (velocity) (Villars and Weisskopf, 1954; Tatarskii, 1971; Hocking, 1985), this relationship has as yet not been well clarified.

2. Description of the Problem

The MST radar observation that is the focus of this study is based on radar tracking of the radar echo due to RRI irregularities or perturbations, with the size along the radar beam being equal to half the radar wavelength for back-scattering. The irregularity is produced by atmosphere turbulence that results from gravity wave breaking in background winds or local winds. In this context, a basic understanding of how the RRI is perturbed in the MST region is required.

RRI, n , consists of three atmospheric elements as

$$n = 1 + 3.73 \cdot 10^{-1} (h/T^2) + 7.76 \cdot 10^{-5} (P/T) - (N_e/2N_c) \quad (1)$$

where the second term in the right-hand side is humidity, with h denoting the partial pressure of water vapor in millibars and T denoting the temperature in Kelvin, the third term is the neutral atmosphere density, with P denoting the pressure expressed in millibars, and the fourth term is the plasma density, with N_e denoting the electron number density per cubic meter and N_c denoting the critical plasma density (given as $N_c = 1.24 \cdot 10^{-2} f^2$ per m^3 with a radio-wave frequency of f per second). The standard atmosphere model gives a height-profile of n (Hasiguchi, 1995; Fig. 1), which decreases from ground level up to about 60 km mainly due to the second and third terms and then increases up to 100 km mainly due to the fourth term; n is minimum at heights between 30 and 60 km. Although these values imply that the radar echo is normally barely detectable in this latter height range, Maekawa *et al.* (1993)

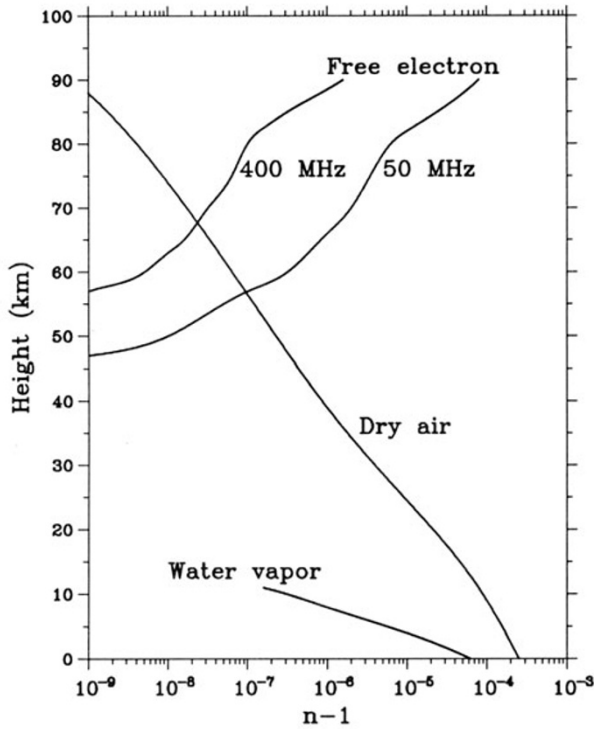


Fig. 1. Height profile of $(n - 1)$ for humidity, density (dry air) and electrons (Hasiguchi, 1995). The radio refractive index with electrons depends on radiowave frequency and illustrates two cases as 400 MHz (Arecibo Radar) and 50 MHz (Jicamarca Radar).

demonstrated that the giant Jicamarca radar can detect turbulence echoes by a long-time integration of the radar echo for several minutes.

The air density perturbation, which corresponds to the third term in Eq. (1) cannot be related to dynamics through an adiabatic variation of pressure since the adiabatic variation is inconsistent with $\text{div } V = 0$, which is assumed in the isotropic turbulence theory as established by Kolmogoroff, Heisenberg, Batchelor and others (Batchelor, 1953). Such an inconsistent approach for producing density perturbation by turbulence (Villars and Weisskopf, 1954; Tatarskii, 1971) has now been revised and a correct approach will be found.

3. RRI Perturbation by Turbulence

Atmospheric density perturbation is, as intuitively understood, produced by the transport of air particles by turbulence velocity V along the vertical gradient in the hydrostatic equilibrium atmosphere. Even with $\text{div } V = 0$ the density perturbation takes place, as given by the equation of continuity

$$\frac{\partial \rho}{\partial t} = -\nabla(\rho V) = -V_z \frac{d\rho_0}{dz} + (\text{second-order small terms}) \quad (2)$$

where V_z is the vertical (positive-upward) turbulence velocity component, $(d\rho_0/dz)$ is the hydrostatic-equilibrium term, which is equal to $(-\rho_0/H)$, with ρ_0 being the background density, and H the scale height assumed to be con-

stant. Integration of Eq. (2) with respect to time during τ , approximately, gives

$$\underline{\delta\rho}(t, \kappa)^2 \propto \underline{V_z}(t, \kappa)^2 \tau^2 \quad (3)$$

where $\delta\rho(t, \kappa)$ the perturbation of air density relative to ρ_0 and $V_z(t, \kappa)$ are the Fourier κ component dependent on t ; τ is an integration time that is comparable to the turbulence correlation time; the underlining denotes the time-average. Equation (3) implies simply that the density perturbation intensity is proportional to $\underline{V_z}^2$ and that the density perturbation spectrum function must be the same with respect to the power spectrum of $\underline{V_z}^2$. We now resort to the established theory of isotropic turbulence. Only isotropic turbulence is theoretically understood. Isotropic turbulence means $\underline{V_x}^2 = \underline{V_y}^2 = \underline{V_z}^2$ whose power spectrum depends only on wave-number magnitude κ , $E(\kappa)$, such that

$$E(\kappa) \propto \kappa^{-5/3} \quad \text{in the inertia sub-range} \quad (4)$$

$$E(\kappa) \propto \kappa^{-7} \quad \text{in the viscous sub-range.} \quad (5)$$

We need not enter further into turbulence theory since our concern is mainly on RRI perturbation in production and motion, not on turbulence dynamics.

The humidity perturbation of the second term in the right-hand side in Eq. (1) is transported in a similar manner as the density perturbation and the spectrum is similar to $\delta\rho$. Our understanding of the co-movement of $(\delta\rho)$ with turbulence is clear, with the equation of continuity in the form of following the motion (e.g. Holton, 1992), such that

$$\frac{D\rho}{Dt} = -\rho \text{div } V = 0 \quad (6)$$

The equation shows that the air mass moves with the flow (by turbulence and winds), maintaining the initial density, as shown in Eq. (3), irregardless of any ambient density distribution. Only in the presence of the vertically gradient distribution of the ambient density can any density perturbation be detected. Note that $\text{div } V = 0$ is essential for the density-perturbation transported with turbulence plus winds (winds are divergence-free). Observations made with radars and radio-sondes are consistent with the theoretical expectation (Luce *et al.*, 2001).

The mesospheric situation is different in that electron density perturbation in the fourth term in Eq. (1) takes place mainly at heights above 60 km, as shown in Fig. 1. Electrodynamic considerations are required for turbulence transportation along $dN_e/dz > 0$ instead of $d\rho_0/dz < 0$ as only electrons are responsible for the radiowave scattering. Whilst ions co-move fairly well up to 120 km, with neutral particles in turbulent motion through collisions, electrons are strongly controlled by the geomagnetic field B_0 above 70 km since the ratio between collision frequency and gyro-frequency $R_{i,e}$ is very different between ions (R_i) and electrons (R_e) in this altitude region. R_i drops to unity at a height 120 km but R_e reaches this level at a much lower height ~ 60 km; $R_{i,e}$ decreases almost exponentially as ρ_0 with heights (Kato, 1980a). Thus, electrons are unable to co-move with the ions as well as neutral particles in the absence of any static gradient of N_e , the density, which plays

a role in producing an electric polarization field E_p that inhibits the control of geomagnetic field. Favorably, as shown in Fig. 1, during the daytime, such a static vertical gradient of N_e exists above 60 km (Rastogi and Bowhill, 1976; Lehmacher *et al.*, 2006). Consequently, electrons can co-move with ions vertically. The details are as follows: as $\delta\rho$, δN_e is produced similarly by Eqs. (2) and (3) in the first-order magnitude as proportional to V_z . Modification of δN_e in the second order small magnitude due to $V \cdot [\text{grad}(\delta N_e)]$ does not significantly affect δN_e intensity, but does significantly affect E_p , which is modified considerably by the second modification on δN_e , as understood in electromagnetic theory (Kato, 1965), to ultimately reach

$$E_p + V \times B_0 = 0. \quad (7)$$

with

$$V_i = V_e = V \quad (8)$$

where $V_{i,e}$ are the velocity of the ions and electrons, respectively, and

$$V_{i,e} = [\xi_{i,e}](E_p + V \times B_0) + V \quad (9)$$

where $[\xi_{i,e}]$ represents the mobility tensors for ions and electrons, respectively, which are dependent on $R_{i,e}$ (Kato, 1980a); E_p is produced and maintained in stationary state with $\text{div } J = 0$, where $J = \text{electric current density}$. Even with a slight inequality between N_e and N_i , as $|N_e - N_i| \ll N_e$, a large E_p is set up, following the Maxwell equation as

$$\text{div } E_p = (N_i - N_e)e/\epsilon_0 \quad (10)$$

in which e is the electron charge and ϵ_0 the vacuum permittivity; $\epsilon_0 = 8.854 \cdot 10^{-12}$ farad/m. If we consider a situation of the mesosphere and a VHF radar, $|\text{div } E_p| \sim |E_p|/L$, where $L = 5$ m, and $(N_i - N_e) = 10^5/\text{m}^3 = 10^{-3}N_e$ at $z = 70$ km. Using Eq. (10), we obtain $E_p = 1$ mV/m, which is consistent with $V = 10$ m/s in Eq. (7).

An additional complication is that in the presence of E_p , Hall drifts proportional to $(E_p \times B_0)$ take place (Kato, 1980a), driving electrons and ions with different velocities and orthogonally to both E_p and B_0 . However, the drifts themselves have no divergence as $\text{div}(E_p \times B_0) = 0$; the drifts are also orthogonal to $[\text{grad}(N_e + \delta N_e)]$. Hence, no additional electron density perturbation occurs. We thus understand that RRI perturbation (δn) in the mesosphere co-moves with turbulence eddies which, in turn, co-move with local winds. Also, the (δN_e) produced suffers no loss due to ionosphere recombination whose rate is much slower than that of turbulence correlation time as a few seconds (Kato, 1980a). Thus, we obtain another relation than that of Eq. (6) for N_e in the form of following the flow

$$\frac{DN_e}{Dt} = -N_e \text{div } V_e = 0 \quad (11)$$

which is based on Eq. (8); as such, the recombination loss is neglected in Eq. (11) as justified above. Further, including humidity in Eq. (1) we have

$$\frac{Dn}{Dt} = 0 \quad (12)$$

RRI irregularities move mainly with the winds, fluctuating with turbulence. This results in the radar echo with the Doppler spectrum, whose central peak corresponds to winds, with the skirts spreading by turbulence and the intensity being dependent on the vertical total flow.

4. Observation of Turbulence with Radars

In addition to tracking turbulence as wind-tracers, MST-radar observations are important tools for studying atmospheric turbulence dynamics.

Radars can detect echoes due to the scattering of turbulence, with the size of half the radar wavelength in heights lower than the critical height where $2k = \kappa_d$, in which k denotes the radar wave-number and κ_d gives the minimum scale of turbulence or the boundary between turbulence inertial subrange and viscous subrange (see Eqs. (4) and (5)). $\kappa_d = (\epsilon/\mu^3)^{1/4}$, where $\epsilon = \text{total power supplied from outside per unit time and unit mass for maintaining the turbulence system}$; $\mu = \text{kinematic viscosity}$. κ_d decreases almost exponentially with height in a manner almost proportional to air density. Thus, we can obtain the distribution of the critical height or the minimum scale of turbulence, as illustrated in Fig. 2 (Balsley and Gage, 1980). A fairly good fitting illustrated in Fig. 2 shows that the radar observation is consistent with the isotropic turbulence theory in which $\lambda_{\min} \approx 2\pi/\kappa_d$ (different from the observation showing a factor 5.92 instead of 2π). Figure 2 contains certain errors about the maximum attainable height of the Jicamarca radar as 50 km, considering 50 MHz of the radar frequency or 6 m of the radar wavelength. This error should be due to n , which is very small around 60 km as in Fig. 1, and not due to the absence of any turbulence eddies corresponding to the half wavelength of the Jicamarca radar. In actual fact, radar echoes were obtained at a height of 75 km, although

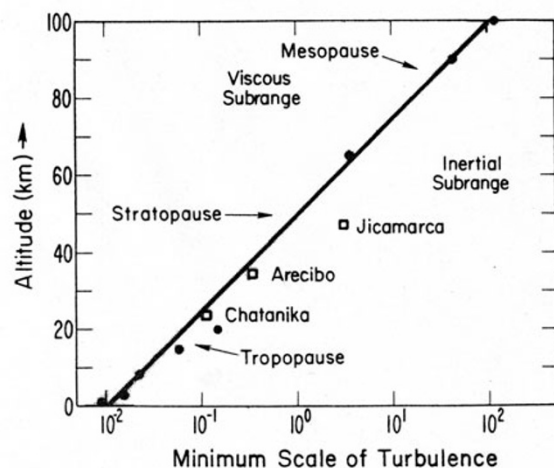


Fig. 2. Minimum scale of turbulence $\lambda_{\min} = 5.92/\kappa_d$ in meters (Balsley and Gage, 1980), dividing turbulence power spectrum into the inertial and viscous subrange. The solid circles and the open squares denote the maximum height of observed atmospheric echoes for radars operating at different frequencies. The open squares are used for particularly well-known radars, with their locations. For the Jicamarca observation, the upper limit height is apparently low due to small n , failing to show the turbulence minimum size corresponding to wavelength (see text).

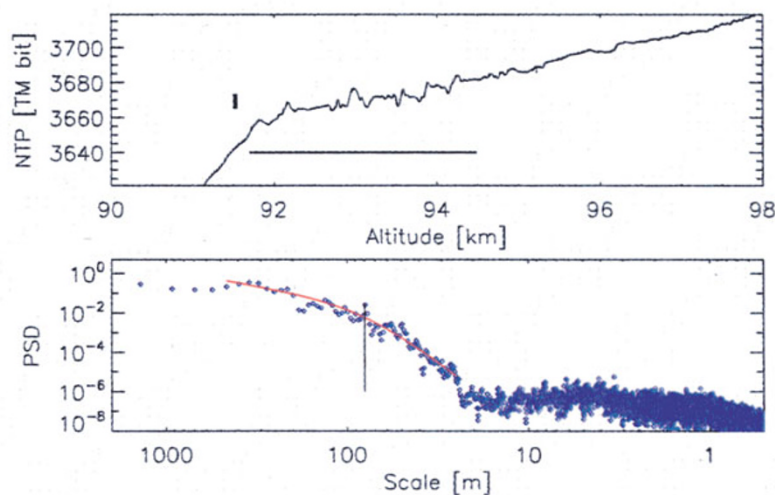


Fig. 3. Top: electron density fluctuation observed by rocket-borne Langmuir probe, September 19, 2004. The rocket launching site was on the Kwajalein Atoll, Marshall Islands. The small vertical bar indicates a fluctuation of 10%. Bottom: power spectrum of the fluctuations over heights shown by the horizontal line (top). The red line is the best fit of $E(\kappa)$ (see Eqs. (4) and (5) in text). The vertical line is located at 80 ± 10 m, showing $9.9/\kappa_d$. The minimum scale of turbulence in inertial subrange is a little longer than that in Fig. 2, giving $\lambda_{\min} = 5.92/\kappa_d$.

these are not shown in Fig. 2 (Woodman and Guillen, 1974; Maekawa *et al.*, 1993). Further, it is possible to derive a turbulence dissipation energy rate ε from $\kappa_d = (\varepsilon/\mu^3)^{1/4}$ where κ_d is obtained from observation, as in Fig. 2, and μ from models (Kato, 1980b); $\varepsilon = 0.5\text{--}1.0$ W/kg at a height of 100 km.

In addition to radar observations, an important in situ observation has recently been performed, obtaining a turbulence spectrum of the electron density (Fig. 3; Lehmacher *et al.*, 2006). This electron density was deduced from the electron density measurement of the Langmuir probe onboard the rockets although the electron density was also measured by incoherent scatter radar by the Altair radar at the Kwajalein Atoll and by the Faraday rotation in radio transmission between the ground and the rockets. Figure 3 gives their electron density perturbation spectrum, which is identified with $E(\kappa)$ in Eqs. (4) and (5) over fairly wide range of κ in both the inertial and viscous sub-range, both of which are bounded at about 80 ∓ 10 m in scale. Note that the boundary between the observed inertial and viscous subrange has a scale of $(5.92/\kappa_d)$ in Fig. 2 and $(9.9/\kappa_d)$ in Fig. 3; as such both are different from $(2\pi/\kappa_d)$, as theoretically expected. The observation gives an ε of to 0.1–0.3 W/kg at heights of 92–94 km, which is consistent with that obtained from Fig. 2.

5. Conclusion

The RRI perturbation (δn) responsible for the MST radar echo is produced in the presence of static vertical gradients of RRI that depend on three properties—humidity, air density and electron density. Turbulence vertical velocity transports those elements along the gradients, producing δn , which moves with the total air flow as turbulence plus winds. Theoretically, the echo power spectrum should be the same as the vertical turbulence velocity spectrum with $\kappa = 2k$; i.e. the eddy size equals half the radar wavelength.

The co-movement takes place because of the divergence-free characteristics of turbulence and is valid even in the mesosphere, where electrons are the main component of RRI and under electromagnetic control. Based on observations, the turbulence κ -spectrum is the same as the isotropic turbulence κ -spectrum, implying that the turbulence produced by gravity waves in breaking may be either isotropic or anisotropic in nature but that the turbulence spectrum is the same as that of the isotropic turbulence spectrum.

Acknowledgments. The author is grateful to Drs. T. Ogawa, D. Fritts and W. Hocking for their comments.

References

- Balsley, B. B. and K. S. Gage, The MST techniques: potential for middle atmosphere studies, *Pure Appl. Geophys.*, **118**, 452–493, 1980.
- Batchelor, G. K., *The theory of homogeneous turbulence*, pp. 46 and 114–132, Cambridge Monograph on Mechanics and Applied Mathematics, Cambridge Univ. Press, 1953.
- Hasiguchi, H., Development of an L-Band clear-air Doppler radar and its Application to planetary boundary layer observations over equatorial Indonesia, p. 10, PhD thesis, Kyoto University, January, 1995.
- Hocking, W. K., Measurements of turbulent energy dissipation rates in the middle atmosphere by radar techniques, A review, *Radio Sci.*, **20**, 1403–1422, 1985.
- Holton, J. R., *An introduction to dynamic meteorology (3rd edition)*, p. 47, Academic Press, San Diego, New York, Boston, London, Sydney, Tokyo, Toronto, 1992.
- Kato, S., Theory of movement of irregularities in the ionosphere, *Space Sci. Rev.*, **4**, 223–235, 1965.
- Kato, S., *Dynamics of the upper atmosphere*, (a) pp. 141–150 (b) pp. 213–215, Center Acad. Publ/D. Reidel Publ, Japan/Dordrecht, Boston, London, 1980.
- Kato, S., Middle atmosphere research and radar observation, *Proc. Jpn. Acad. Ser. B*, **8**, 306–320, 2005.
- Lehmacher, G. A., C. L. Croskey, J. D. Michell, M. Friedrich, F.-J. Lueben, M. Rapp, E. Kudeki, and D. C. Fritts, Intense turbulence observed above a mesospheric temperature inversion at equatorial latitude, *Geophys. Res. Lett.*, **33**(8), L08808, 2006.
- Luce, H., S. Fukao, M. Yamamoto, C. Sidi, and F. Dalaudier, Validation of winds measured by GPS radiosondes during the MUTSI Campaign, *J. Atmos. Oceanic Tech.*, **18**, 817–829, 2001.

- Maekawa, Y., S. Fukao, M. Yamamoto, M. D. Yamanaka, T. Tsuda, S. Kato, and R. F. Woodman, First observation of the upper stratospheric vertical wind velocities using the Jicamarca VHF radar, *Geophys. Res. Lett.*, **20**, 2235–2238, 1993.
- Rastogi, P. K. and S. A. Bowhill, Scattering of radio waves from the mesosphere-2, Evidence for intermittent mesospheric turbulence, *J. Atmos. Terr. Phys.*, **38**, 449–462, 1976.
- Tatarskii, V. I., *The effect of the turbulent atmosphere on wave propagation*, National Technical and Information Service, pp. 74–76, Springfield, Va, 1971.
- Villars, F. and V. F. Weisskopf, The scattering of electromagnetic waves by turbulent atmospheric fluctuations, *Phys. Rev.*, **94**, 232–240, 1954.
- Woodman, R. F. and A. Guillen, Radar Observation of Winds and Turbulence of the Stratosphere and Mesosphere, *J. Atmos. Sci.*, **31**, 493–505, 1974.

S. Kato (e-mail: kato@rish.kyoto-u.ac.jp)